Laser and Particle Beams (2014), *32*, 429–435.

doi:10.1017/S0263034614000330

Plasma plume behavior of laser ablated cerium oxide: Effect of oxygen partial pressure

ARUN KUMAR PANDA,[1] AKASH SINGH,[1] MANEESHA MISHRA,[1] R. THIRUMURUGESAN,[1] P. KUPPUSAMI,[2] AND E. MOHANDAS[1]

[1]Materials Synthesis and Structural Characterisation Division, Physical Metallurgy Group, Indira Gandhi Centre for Atomic Research, Kalpakkam, India
[2]Centre for Nanoscience and Nanotechnology, Sathyabama University, Chennai, India

(RECEIVED 26 December 2013; ACCEPTED 7 May 2014)

Abstract

This paper describes the spatial and temporal investigation of laser ablated plasma plume of cerium oxide target using Langmuir probe. Cerium oxide target was ablated using a KrF (λ ~ 248 nm) gas laser. Experimental studies confirmed that oxygen partial pressure of 2×10^{-2} mbar is sufficient enough to get good quality films of cerium oxide. At this pressure, plume was diagnosed for their spatial and temporal behavior. Spatial distribution was investigated at a distance of 15 mm, 30 mm, and up to a maximum distance of 45 mm from the target, whereas temporal behavior has been recorded in the range of 0 to 50 μS with an interval of 0.5 μS. The average electron densities are found to be maximum at 30 mm from the target position and the plasma current of the laser ablated ceria is found to be maximum at 22 μS.

Keywords: Cerium oxide; Langmuir probe; Plasma; Pulsed laser deposition

INTRODUCTION

Pulsed laser deposition is the simplest physical vapor deposition technique for the synthesis of complex-oxide hetero structures, multilayers, and well-controlled interfaces in thin films. The method offers excellent control on stoichiometric transfer of material from the target to substrate and has good compatibility on working with background pressures ranging from ultrahigh vacuum to 1 Torr (Eason, 2007). The pulsed laser deposition equipment is flexible as the energy source creating the plume is separated from the deposition system (Boyd, 1996; Baron *et al*., 1993; Dogar *et al*., 2011). The laser produced plasmas are non-equilibrium and non-thermal (Dogar *et al*., 2011; Chrisey & Hubler, 1994), which have found important application in various research fields such as material growth and processing which include deposition of thin films, synthesis of nano-particles and elemental analysis of multi component materials (Baron *et al*., 1993; Dogar *et al*., 2011). When nanosecond pulsed laser radiation is absorbed by a solid target, the electromagnetic energy is converted into electronic excitation and it heats, melts, and vaporizes the target (Chrisey & Hubler, 1994). These ablated species form a plasma plume containing mixture of atoms, molecules, electrons, and ions (Chrisey & Hubler, 1994; Doggett & Lunney, 2009; Lenk *et al*., 1996; Merlino, 2007; Singh & Narayan, 1990; Zheng *et al*., 1989; Wood & Giles, 1981; Caridi *et al*., 2008). The plasma plume expands with supersonic velocity (Singh & Narayan, 1989) and its parameters such as plasma temperature, ion density, electron density, electron temperature vary with laser parameters such as frequency, energy irradiance as well as on the background pressure (Inam *et al*., 1987; Neifeld *et al*., 1988). The laser produced plasma is highly transient in nature and its parameters vary in both space and time. The studies of spatio-temporal evolution of plasma plays an important role during thin film synthesis as it provides information about various processes occurring during the formation and expansion of plasma. The plasma characteristics have a direct bearing on the kinetics and quality of thin films. Langmuir probe is used as a diagnostic tool to get insight on behavior of laser produced plasma. It is the simplest electrical probe technique used to measure the plasma parameters of low temperature laboratory plasma and also applicable to transient plasma (Dogar *et al*., 2011;

Address correspondence and reprint requests to: Arun Kumar Panda, Materials Synthesis and Structural Characterisation Division, Physical Metallurgy Group, Indira Gandhi Centre for Atomic Research, Kalpakkam-603 102, India. E-mail: akpanda@igcar.gov.in

Kumari *et al.,* 2012; Doggett & Lunney, 2009; Hong *et al*., 2000; Toftmann *et al*., 2000). The probe tip is inserted along the length of the plasma to collect the ions and electrons effectively and tip chosen is very thin so that there is no perturbation to the plasma plume. A variable voltage is applied to the tip and the corresponding current (electrons and ions) is collected (Neifeld *et al*., 1988). All the plasma parameters were measured from the I-V characteristic of the probe. Cerium oxide has been of great interest due to high refractive index (2 at 500 nm), high melting point (2873 K), large dielectric constant (~26) (Patsalas *et al*., 2002), wide band gap (3.6 eV), high transparency in the visible-near infrared regions, chemical stability, good adhesion, high hardness, and thermal stability (Inoue *et al*., 1991; Elidrissi *et al*., 2000; Kanakaraju *et al*., 1997). It can be used as ultra violet blocking filters, single and multilayer coatings for optical devices (Rao *et al*., 2003) and electrochromic windows due to wide band gap and good transparency in visible-near infrared regions. Ceria thin film is used in random access memory, colossal magneto resistance, ferroelectrics, ultrathin gate oxide for complementary metal oxide semiconductor technology, stable capacitor devices for large scale integration (Luo *et al*., 1991), and corrosion protection coatings of metals and alloys. Also, there are few published reports in which synthesis of ceria thin films have been carried out using pulsed laser deposition (Wang *et al*., 1999; Sanchez *et al*., 1993; Hirschauer *et al*., 1999; Li *et al*., 1998; Cossarutto *et al*., 1998; Balakrishnan *et al*., 2009; Kuppusami *et al*., 2005). The hyper thermal species (neutral cerium oxygen atoms and ions) generated by pulsed laser deposition plays an important role in increasing the adatom mobility and film quality because they have high value of kinetic energy of the order of 5–100 eV. Hence, detailed study of spatial variation of ion density and average energy of ionized species under different pressure is important for synthesis of good quality thin films with an understanding of the formation process. In the present work, we have reported the effect of oxygen pressure on the ion density and average energy of ionized species (cerium and oxygen ions) to understand the plasma dynamics during film synthesis.

EXPERIMENTAL SETUP

Cerium oxide powder of 99.99% purity (Alpha Aesar) was fine ground and compacted to a pellet of 20 mm diameter and 3 mm thickness by applying a pressure of 10 MPa. The pellet was sintered at 1693 K for 4 hr and the sintered density was calculated and found to be about 90%. The pellet was characterized by an INEL XRG-3000 X-ray diffractometer attached with a curved position sensitive detector using Cu Kα1 (0.15406 nm) radiation. The ceria pellet was cleaned with acetone and mounted onto the target holder located inside a vacuum chamber using silver paste. The chamber was evacuated to 10^{-5} mbar by Alcatal rotary and turbo molecular pumps. The oxygen partial pressure inside the chamber was controlled by a MKS make mass flow controller. The oxygen partial pressure was varied from 10^{-2} to 10^{-5} mbar. The plasma parameters were diagnosed by an automated Langmuir probe (ALP; IMPEDANS, Ireland) in both space and time resolved mode. The probe consists of a tungsten tip of diameter of 0.39 mm mounted in a ceramic coated probe shaft made up of alumina so that it can sustain heat loads from the plasma. Spatial plasma measurement was carried out by an ALD. The ALD facilitates the movement of probe tip from target position to the substrate position using a stepper motor via the RS 232 system. The laser produced plasma is time dependent and the temporal variation was investigated by suitably choosing the time duration of 0 to 50 μs with an interval of 0.5 μs in Langmuir probe software. The time resolved mode in the Langmuir probe works in an advanced boxcar mode. The rising edge of the synchronized signal of the pulsed laser triggers the data acquisition. The clock (12.5 ns sample time) of the detection circuit ensures that each time step is recorded accurately. The advanced boxcar mode gives the advantages of a level triggered gate mode while retaining the highest level of time accuracy. Typical experimental set-up is shown in Figure 1. A KrF excimer laser (Lambda Physik, Compex-205) of 248 nm wavelength was used as the energy source with energy of 300 mJ/pulse, repetition rate of 10 Hz, and pulse duration of 25 ns for ablating the cerium oxide. The laser light was focused onto the target using a cylindrical lens of focal length 50 cm. The base pressure was varied from 10^{-5} to 10^{-2} mbar by flowing the oxygen gas in the background. The optimized oxygen partial pressure of 2×10^{-2} mbar (Balakrishnan *et al*., 2009; 2011) to get high quality thin films for CeO_2 was used in most of the experiments in the present work. The experimental conditions used for the deposition of ceria have already been reported (Balakrishnan *et al*., 2009; 2011). The temporal variation of plasma was investigated by placing the ALP at a position of about 30 mm from the target normal to the target-substrate distance. The plasma current was collected for 50 μs with a time step of 0. 5 μs.

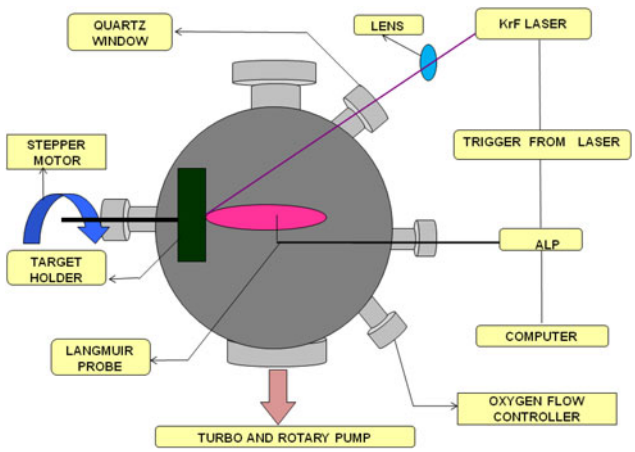

Fig. 1. (Color online) Schematic Experimental Set up of Pulsed Laser Deposition unit fitted with automated Langmuir probe.

https://doi.org/10.1017/S0263034614000330 Published online by Cambridge University Press

The spatial variation of plasma parameters were studied at the oxygen partial pressure of 10^{-2} mbar as a function of probe distance from the target. This was carried out by placing the probe tip at 0, 15, 30, and 45 mm from the target. The probe voltage was varied from −20 to +35 V and the corresponding plasma current was collected by the Langmuir probe. The plasma parameters such as plasma temperature, ion density, electron density, and electron temperature were calculated from the I versus V plot using ALP software.

RESULTS AND DISCUSSION

X-ray diffraction measurement was carried for CeO_2 pellet to confirm the phase purity as it will be used as a pulsed laser deposition target for plasma diagnostics. Figure 2 shows the X-ray diffraction pattern which indicates all the reflections from ceria (JCPDS-340394) belonging to face centered cubic structure and there was no impurity present in the target. The temporal variation of plasma current at different probe voltages of 5, 10, and 15 V at the substrate position of 30 mm at the oxygen partial pressure of 10^{-2} mbar was measured using the ALP and is shown in Figure 3. The plasma current is found to be maximum at 22 μs and the plasma tends to die out inside the chamber after 22 μs. A typical probe current (I) versus probe voltage (V) at 22 μs is shown in Figure 4, which is a screen shot of the ALP system. The floating potential and plasma potential are found to be −0.45 V and 6.20 V, respectively. The plasma parameters were calculated from the I − V plot which are shown in Table 1. At large negative bias voltage (≤5 V), the electrons are repelled because of Coulomb repulsion and negative voltage is high enough to prevent the electrons with the highest thermal energy in the plasma from reaching the probe so that the probe is saturated with ions giving rise to ion saturation current region represented as "A" in the Figure 4. As the probe is made slightly negative at −0.45 V, floating potential V_f is reached, where electron

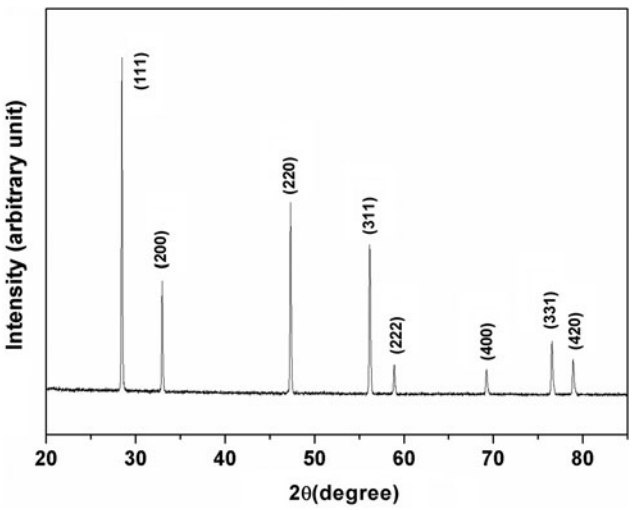

Fig. 2. XRD Pattern of CeO_2 pellet sintered at 1693 K, 4 hr.

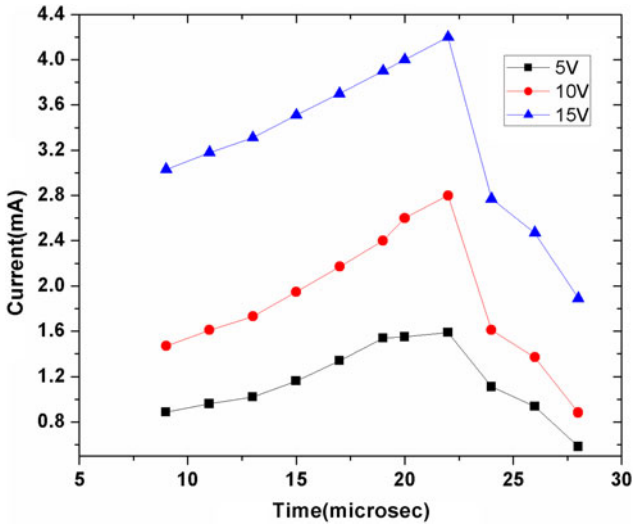

Fig. 3. (Color online) Temporal Variation of plasma current of CeO_2 plasma plume as a function of probe voltage at the substrate position of 30 mm at the oxygen partial pressure of 10^{-2} mbar.

and ion currents are equal in magnitude. With increase in the probe voltage beyond V_f, there is a transition region where probe with positive voltage collects more electrons than ions up to plasma potential, V_p of 6.20 V. In this regime, the potential barrier between the probe and plasma decreased and became 0 at V_p. This region is known as electron retardation region as shown as "B" in Figure 4. To the right of V_p, the positive probe potential attracts electrons and there is a region of electron saturation which is represented as the region "C" (electron saturation region) in the figure above. The electron saturation region with error bars was calculated by ALP software taking care of sheath expansion incorporating Laframboise and Druyvesteyn theory (Laframboise, 1966; Druyvesteyn, 1930). The inset of Figure 4 shows a semi-logarithmic plot of the I-V curve for the probe distance of 30 mm from the target. Probe bias voltage data points were fitted linearly to confirm the electron saturation and their intersection gives the value of plasma potential of 6.20 V. The pressure was varied from 10^{-2} to 10^{-5} mbar by flushing oxygen gas into the chamber. The plasma parameters like electron temperature (Chen, 1974; Klagge & Tichy, 1985), electron flux, ion flux, ion density (Talbot *et al.*, 1966; Zakrzewski & Kopiczynski, 1974; Rousseau *et al.*, 2005), average electron density, average energy (Allen *et al.*, 1957; Hopkins, 1995; Boyd & Twiddy, 1959; Druyvesteyn, 1930; Allen, 1992), and average electron temperature (Hopkins, 1995; Laframboise, 1966) were measured from the I-V plot using the ALP software. All plasma parameters are measured by Langmuir probe assuming cerium and oxygen ions are single ionized (Doggett & Lunney, 2009; Toftmann *et al.*, 2000). The variation of ion density with pressure is shown in Figure 5. From Figure 5, it is clear that the ion density of cerium and oxygen decreased with increase in pressure which was found to have a maximum value of $2.25 \times 10^{17} m^{-3}$ at 10^{-5} mbar and a minimum

https://doi.org/10.1017/S0263034614000330 Published online by Cambridge University Press

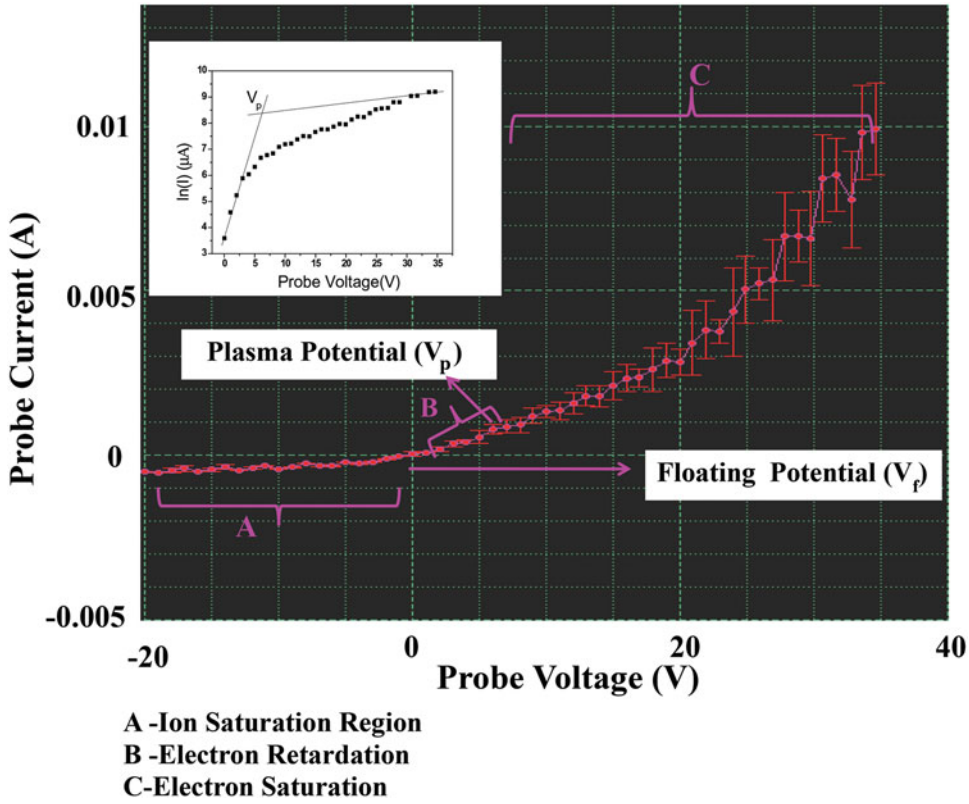

Fig. 4. (Color online) Typical probe current Vs voltage at a time of 22 μs.

Table 1. *Plasma parameters of the ceria plume at a distance of 30 mm from the target*

Plasma Potential, V_P (V)	6.20 ± 0.0576
Floating Potential, V_F (V)	-0.45 ± 0.0054
Electron Temperature, kT_e (eV)	12.9 ± 0.2322
Electron Flux, J_e (A/m^2)	453 ± 9.966
Electron Density, N_e (m^{-3})	$5.05 \times 10^{15} \pm 9.595 \times 10^{13}$
Ion Flux, J_p (A/m^2)	16.8 ± 0.3528
Ion Density, N_i (m^{-3})	$7.05 \times 10^{15} \pm 1.6215 \times 10^{14}$
Average Electron Density N_e (m^{-3})	$1.26 \times 10^{16} \pm 3.27 \times 10^{14}$
Average Energy, E (eV)	9.91 ± 0.2576
Average Electron Temperature, kT_e (eV)	6.61 ± 0.0793

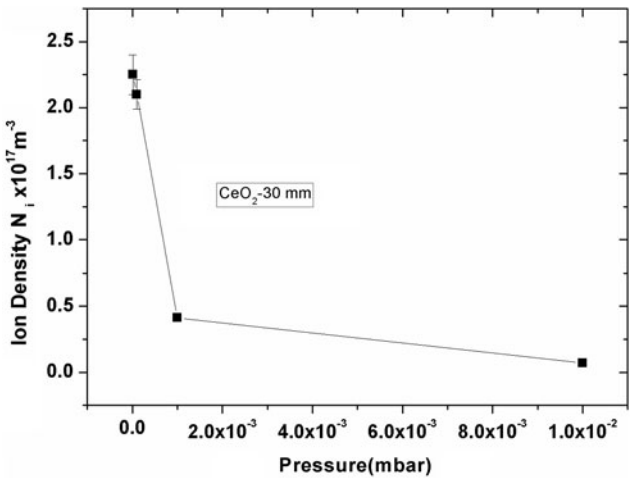

Fig. 5. Variation of ion density with oxygen partial pressure during pulsed laser deposition of ceria.

of $7.05 \times 10^{15}/m^{-3}$ at 10^{-2} mbar. The decrease in the ion density with increasing oxygen partial pressure is attributed to the enhanced recombination of neutral oxygen atoms in forming oxygen molecules. As the oxygen partial pressure is increased, the plasma gets confined which enhances the elastic and inelastic collisions of cerium and oxygen ions with neutral oxygen molecules leading to recombination. As a result of which, the density of cerium and oxygen ions decreased with the increase in the oxygen partial pressure. The variation of average energy of ionized species of cerium and oxygen as a function of oxygen partial pressure is shown in Figure 6, which indicates that the average energy increases with increase in pressure. The average energy of ionized ceria is found to be 6.06 eV at 10^{-5} mbar and 9.91 eV at 10^{-2} mbar with the intermediate values of 6.07 eV and 6.34 eV at 10^{-4} and 10^{-3} mbar, respectively. The increase in average energy with pressure is due to the gain of energy from recombination and the frequent collision of cerium ions with neutral oxygen molecules. The higher value of average energy of 9.91 eV of ionized species at 10^{-2} mbar could enhance the adatom

https://doi.org/10.1017/S0263034614000330 Published online by Cambridge University Press

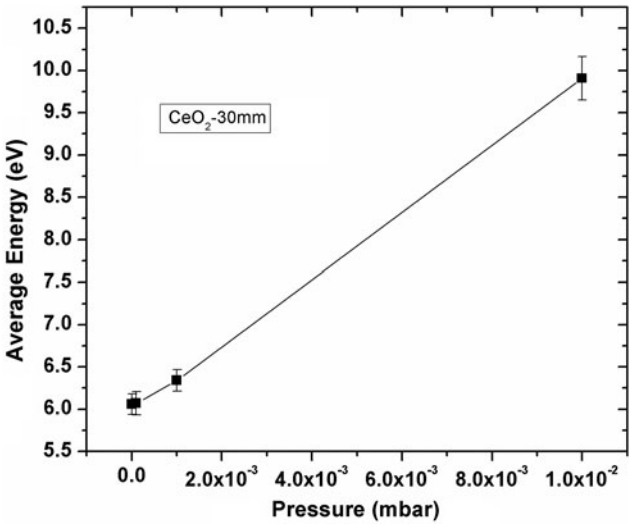

Fig. 6. Variation of average energy with oxygen partial pressure.

mobility for synthesis of good quality ceria thin films compared to average energy of ionized species at lower pressure. This result is consistent with earlier report given by our group (Balakrishnan *et al*., 2009; 2011). The current results also confirm on the structural correlation between the average energy of ionized species with adatom mobility for synthesis of good quality thin films at the oxygen partial pressure of 10^{-2} mbar.

SPATIAL VARIATION OF PLASMA PARAMETERS AT AN OXYGEN PARTIAL PRESSURE OF 10^{-2} mbar

The spatial variation of plasma parameters were measured at 0, 15, 30, and 45 mm from the target by moving the probe tip from the target position to a distance of 45 mm with a step of 15 mm at the oxygen partial pressure of 10^{-2} mbar. The spatial variation of ion density of ceria at 10^{-2} mbar is

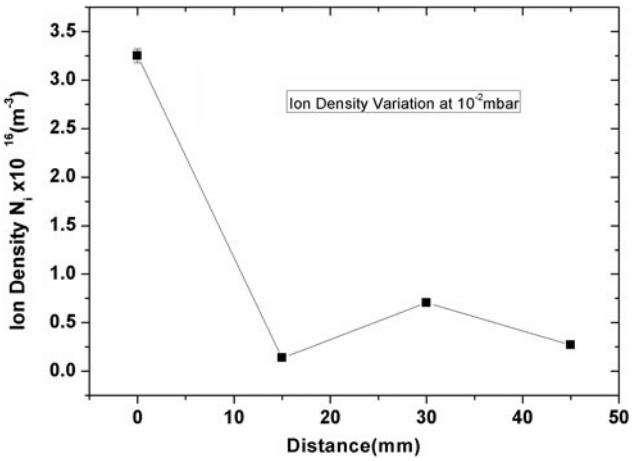

Fig. 7. Spatial variation of ion density at the oxygen partial pressure of 10^{-2} mbar.

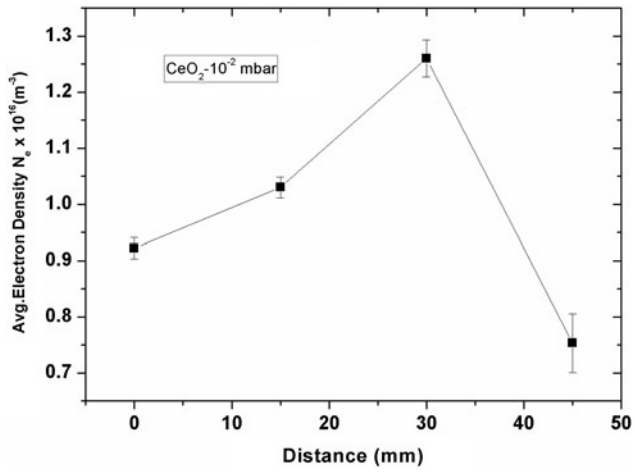

Fig. 8. Spatial variation of average electron density at the oxygen partial of 10^{-2} mbar.

shown in Figure 7. The ion density (3.25×10^{16} m^{-3}) was found to be maximum at the target location and then it decreased to 1.36×10^{15} m^{-3} at 15 mm but the ion density was slightly more (7.05×10^{15} m^{-3}) at a distance of 30 mm from the target. As the plume becomes less dense, the ion density decreased to a value of 2.7×10^{15} m^{-3} at a distance of 45 mm. The average electron density of cerium and oxygen at 10^{-2} mbar was found to be maximum at 30 mm and minimum at 45 mm from the target and it was reported as $1.26 \times 10^{16} m^{-3}$ and $7.53 \times 10^{15} m^{-3}$, respectively. The decrease in both average electron density and ion density at a distance of 45 mm indicates that the plasma plume is more transparent due to increased recombination. It is also noticed from Figures 7 and 8 that the average ion density is higher only close to the target, while the electron density is maximum at a distance of 30 mm. The observation of higher electron density at a longer distance from the target indicates the increased mobility of the electrons compared to ions of cerium and oxygen at this oxygen pressure. From the spatial ion density and average electron density profile, it is clear that plume is transparent beyond the distance of 30 mm because of the dominance of recombination which results the formation of more neutral species. It is clear that distance of 30 mm can be taken as an onset position for the recombination in the present investigation and substrate can be placed at a distance of 30–45 mm from the target which will improve the film quality during the deposition. The measurement of spatial and temporal variation of plasma parameters could lead the better understanding of the plasma formation and expansion of the laser ablated plume of ceria.

CONCLUSIONS

Effect of oxygen partial pressure on plasma parameters have been extensively studied by Langmuir pobe in both spatial and time resolved mode during the pulsed laser deposition

https://doi.org/10.1017/S0263034614000330 Published online by Cambridge University Press

of ceria. The plasma parameters like electron temperature, ion density, average electron density, average energy, and average electron temperature were measured from the I–V plot using the ALP software in the pressure range 10^{-2} to 10^{-5} mbar of oxygen partial pressure. The following are the important conclusions:

- The ion density of cerium and oxygen decreased with increase in the oxygen partial pressure which was found to have a maximum value of $2.25 \times 10^{17} m^{-3}$ at 10^{-5} mbar and a minimum of $7.05 \times 10^{15} m^{-3}$ at 10^{-2} mbar.
- The average energy of the ionized ceria is found to be 9.91 eV at 10^{-2} mbar and 6.06 eV at 10^{-5} mbar with the intermediate values of 6.34 eV and 6.07 eV at 10^{-3} and 10^{-4} mbar, respectively. The increase in the average energy with oxygen partial pressure is attributed to the gain of energy from recombination. The high value of average energy of ionized species increases the adatom mobility for synthesis of good quality of thin films.
- The spatial variation of plasma parameters were measured at different locations between the target and the substrate holder at an oxygen partial pressure of 10^{-2} mbar. The average ion density is higher only close to the target, while the electron density is maximum at a distance of 30 mm. The observation of higher electron density at a longer distance from the target indicates the increased mobilities of the electrons compared to those ions of cerium and oxygen at this oxygen pressure

ACKNOWLEDGEMENTS

The authors are thankful to Dr. M. Vijayalakshmi, Associate Director, Physical Metallurgy Group, Dr. T. Jayakumar, Director, Metallurgy and Materials Group, and Dr. P. Vasudeva Rao, Director, IGCAR for the support and encouragement.

REFERENCES

Allen, J.E., Boyd, R.L.F. & Reynolds, P. (1957). The collection of positive ions by a probe immersed in a plasma. *Proc. Phys. Soc. B.* **70**, 297–304.

Allen, J.E. (1992). Probe theory: The orbital motion approach. *Phys. Scripta* **45**, 497–503.

Balakrishnan, G., Kuppusami, P., Sairam, T.N., Thirumurugesan, R., Mohandas, E. & Sastikumar, D. (2009). Synthesis and properties of ceria thin films prepared by pulsed laser deposition. *J. Nanosci. Nanotechnol.* **9**, 5421–5424.

Balakrishnan, G., Sundari, S.T., Kuppusami, P., Mohan, P.C., Srinivasan, M.P., Mohandas, E., Ganesan, V. & Sastikumar, D. (2011). Study of microstructural and optical properties of nanocrystalline ceria thin films prepared by pulsed laser deposition. *Thin Solid Films* **519**, 2520–2526.

Baron, B., Dubowski, J.J. & Norton, D.P. (1993). Laser ablation in materials processing: Fundamentals and applications. *Mater. Res. Soc. Symp. Proc.* **285**, 501–507.

Boyd, R.L.F. & Twiddy, N.D. (1959). Electron energy distributions in plasmas. *Intern. Proc. Roy. Soc.* **250**, 53–69.

Boyd, I.W. (1996). Thin film growth by pulsed laser deposition. *Ceramics International* **22**, 429–434.

Caridi, F., Torrisi, L., Margarone, D. & Borrielli, A. (2008). Investigation on low temperature laser-generated plasmas. *Lase. Part. Beams* **26**, 265–271.

Chen, F.F. (1974). *Introduction to Plasma Physics*. New York: Plenum Press.

Chrisey, D.B. & Hubler, G.K. (1994). *Pulsed Laser Deposition of Thin Films*. New York: John Wiley & Sons.

Cossarutto, L., Chaoui, N., Millon, E., Muller, J.F., Lambert, J. & Alnot, M. (1998). CeO_2 thin films on Si (100) obtained by pulsed laser deposition. *Appl. Surf. Sci.* **126**, 352–355.

Dogar, A.H., Ilyas, B., Ullah, S., Nadeem, A. & Qayyum, A. (2011). Langmuir Probe Measurements of Nd-YAG laser-produced copper plasmas. *IEEE Trans. Plasma Sci.* **39**, 897–900.

Doggett, B. & Lunney, J.G. (2009). Langmuir probe characterization of laser ablation plasmas. *J. Appl. Phy.***105**, 1–6.

Druyvesteyn, M.J. (1930). Der Niedervoltbogen. *Z Phys A Hadrn. Nucl.* **64**, 781–798.

Eason, R. (2007). *Pulsed Laser Deposition of Thin Films: Applications-Led Growth of Functional Materials*. New Jersey:-John Wiley & Sons.

Elidrissi, B., Addou, M., Regragui, M., Monty, C., Bougrine, A. & Kachouane, A. (2000). Structural and optical properties of CeO2 thin films prepared by by spray pyrolysis. *Thin Solid Films* **379**, 23–27.

Hirschauer, B., Chiaia, G., Gothelid, M. & Karlsson, U.O. (1999). Studies of highly oriented CeO_2 flms grown on Si(111) by pulsed laser deposition. *Thin Solid Films* **348**, 3–7.

Hong, C., Chae, H.B., Lee, S.B., Han, Y.J., Jung, J.H., Cho, B.K. & Park, H. (2000). Langmuir probe measurement of electron density and electron temperature in the early stage of a laser produced carbon plasma. *Trans. Electri. Electronic. Matr.* **1**, 32–39.

Hopkins, M.B. (1995). Langmuir probe measurements in the gaseous electronic conference rf reference cell. *J. Res. Natl. Inst. Stand. Technol.* **100**, 415–425.

Inam, A., Wu, X.D., Venkatesan, T., Ogale, S.B., Chang, C.C. & Dijikamp, D. (1987). Pulsed Laser etching of high T_c superconductor films. *Appl. Phys. Lett.* **51**, 1112–1114.

Inoue, T., Ohsuna, T., Luo, L., Wu, X.D., Maggiore, C.J., Yamamoto, Y., Sakurai, Y. & Chang, J.H. (1991). Growth of (110)-oriented CeO_2 layers on (100) silicon substrates. *Appl. Phys. Lett.* **59**, 3604–3606.

Kanakaraju, S., Mohan, S. & Sood, A.K. (1997). Optical and structural properties of reactive ion beam sputter deposited CeO_2 films. *Thin Solid Films* **305**, 191–195.

Klagge, S. & Tichy, M. (1985). A contribution to the assessment of the influence of collisions on the measurements with Langmuir Probes in the thick sheath working regime. *Czech. J. Phys. Sect. B.* **35**, 988–1006.

Kumari, S., Kushwaha, A. & Khare, A. (2012). Spatial distribution of electron temperature and ion density in laser induced ruby (Al_2O_3:Cr^{3+}) plasma using Langmuir probe. *J. Inst.* **7**, C05017/1–9.

KUPPUSAMI, P., PADHI, S.N., MUTHUKUMARAN, K., MOHANDAS, E. & RAGHUNATHAN, V.S. (2005). Pulsed laser deposition of novel oxide materials. *Surf. Eng.* **21**, 172–175.

LAFRAMBOISE, J.G. (1966). Theory of spherical and cylindrical Langmuir probe in a collision less Maxwellian plasma at rest. Report No.100. University of Toronto.

LENK, A., SCHLTRICH, B. & WITKE, T. (1996). Diagnostics of laser ablation and laser induced plasmas. *Appl. Surf. Sci.* **106**, 473–477.

LI, M.Y., WANG, Z.L., FAN, S.S., ZHAO, Q.T. & XIONG, G.C. (1998). Structural characteristics and the control of crystallographic orientation of CeO_2 thin films prepared by laser ablation. *Nucl. Instrum. Meth. B* **135**, 535–539.

LUO, LI., WU, X.D., DYE, R.C., MUENCHAUSEN, R.E., FOLTON, S.R., COULTER, Y.C., MAGGIORE, J. & INOUE, T. (1991). a-axis oriented $YBa_2Cu_3O_7 - x$ thin films on Si with CeO_2 buffer layers. *Appl. Phys. Lett.* **59**, 2043–2045.

MERLINO, R.L. (2007). Understanding Langmuir probe current-voltage characteristics. *Am. J. Phys.* **75**, 1078–1085.

NEIFELD, R.A., GUNAPALA, S., LIANG, C., SHAHEEN, S.A., CROFT, M., PRICE, J., SIMONS, D. & HILL, W.T. (1988). Systematics of thin films formed by excimer laser ablation: Results on $SmBa_2Cu_3O_7$. *Appl. Phys. Lett.* **53**, 703–704.

PATSALAS, P., LOGOTHETIDIS, S. & METAXA, C. (2002). Optical performance of nanocrystalline transparent ceria films. *Appl. Phys. Lett.* **81**, 466–468.

RAO, K.N., SHIVLINGAPPA, L. & MOHAN, S. (2003). Studies on single layer CeO_2 and SiO_2 films deposited by rotating crucible electron beam evaporation. *Mater. Sci. Eng. B* **98**, 38–44.

ROUSSEAU, A., TEBOUL, E. & BECHU, S. (2005). Comparison between Langmuir probe and microwave autointerferometry measurements at intermediate pressure in an argon surface wave discharge. *App. Phys.* **98**, 083306/1–9.

SANCHEZ, F., VARELA, M., FERRATER, C., GARCIA-CUENCA, M.V., AGUIAR, R. & MORENZA, J.L. (1993). Structural and compositional thin films characterization of laser ablated CeO_2. *Appl. Surf. Sci.* **70**, 94–98.

SINGH, R.K. & NARAYAN, J. (1989). A novel method for simulating laser-solid interactions in semiconductors and layered structure. *J. Mater. Sci. Eng. B* **3**, 217–230.

SINGH, R.K. & NARAYAN, J. (1990). Pulsed-laser evaporation technique for deposition of thin films: physics and theoretical model. *Phys. Rev. B* **41**, 8843–8859.

TALBOT, L.,CHOU, Y.S. & WILLIS, D.R. (1966). Kinetic theory of a spherical electrostatic probe in a stationary plasma. *Phys. Fluids* **9**, 2150–2167.

TOFTMANN, B., SCHOU, J., HANSEN, T.N. & LUNNEY, J.G. (2000). Angular distribution of electron temperature and density in a laser-ablation plume. *Phys. Rev. Lett.* **84**, 3998–4001.

WANG, R.P., PAN, S.H., ZHOU, Y., ZHOU, G., LIU, N., XIE, K. & LU, H. (1999). Fabrication and characteristics of CeO_2 films on Si(100) substrates by pulsed laser deposition. *J. Cryst. Growth* **200**, 505–509.

WOOD, R.F. & GILES, G.E. (1981). Macroscopic theory of pulsed-laser annealing- thermal transport and melting. *Phys. Rev. B* **23**, 2923–2942.

ZAKRZEWSKI, Z. & KOPICZYNSKI, T. (1974). Effect of collisions on positive ion collection by a cylindrical Langmuir probe. *Plasma Phys.* **16**, 1195–1198.

ZHENG, P., HUANG, Z.Q., SHAW, D.T. & KOWK, H.S. (1989). Generations of high energy atomic beams in laser – Superconducting target interaction. *Appl. Phys. Lett.* **54**, 280–282.